16. Radtke M., Reinholz U., Gebhard R. Synchrotron Radiation-Induced X-Ray Fluorescence (SRXRF) Analyses Of The Bernstorf Gold // Archaeometry. 2016. Vol. 59, Issue 5. P. 891–899. doi: https://doi.org/10.1111/arcm.12294
17. Rößiger V., Nensel B. Non destructive analysis of gold alloys using energy dispersive X-ray fluorescence analysis // Gold Bulletin. 2003. Vol. 36, Issue 4. P. 125–137. doi: https://doi.org/10.1007/bf03215503
18. Jurado-López A., de Castro L., Pérez-Morales R. Application of energy-dispersive X-ray fluorescence to jewellery samples determining gold and silver // Gold Bulletin. 2006. Vol. 39, Issue 1. P. 16–21. doi: https://doi.org/10.1007/bf03215528
19. Metodyka vykonannia vymiriuvan masovoi chastky zolota v zoloto-sribnykh, zoloto-midnykh i zoloto-sribno-midnykh splavakh metodom kupeliuvannia: svidotstvo «Ukrmetrteststandart» No. MVV 081/12-0668-09. Kyiv: DPS Minfinu Ukrainy, 2010. 18 p.

Катодним темплатним методом були отримані тонкі плівки гідроксиду нікелю, які надалі випробовувались у різних розчинах. Розчини містили 0,1 М КОН та 0,1 М КОН з додаванням різної кількості K_2WO_4: 0,1, 0,3 та 1 мМ. Випробування плівок показало, що наявність іонів вольфрамату може істотно впливати на електрохімічні та електрохромні характеристики плівок $Ni(OH)_2$. Вихідний зразок, який випробували у розчині 0,1 М КОН, показав відмінності у порівнянні з електрохімічними характеристиками зразків, що випробували у розчинах з 0,1 М КОН та K_2WO_4. Відмінність полягала в значній різниці поміж величинами густин струмів катодного й анодного піків та наявність струмового плато на циклічній вольтамперограмі. При цьому вихідний зразок продемонстрував найвищу серед усіх абсолютну глибину затемнення 74 %. З іншої сторони вихідний зразок мав зростання величини абсолютної глибини затемнення, а потім поступове її зменшення.

У свою чергу зразки, що випробували у розчинах з вольфраматом, мали кращі електрохімічні характеристики – чіткі катодні та анодні піки, що мали більш близькі значення густин струмів. Динаміка зміни абсолютної глибини затемнення для всіх зразків у серії з додаванням вольфраматів мала постійне її збільшення. При цьому зразок випробуваний у розчині з 1 мМ вольфрамату мав найменше значення абсолютної глибини затемнення – 60 %. Для концентрацій вольфрамату 0,1 та 0,3 мМ абсолютна глибина затемнення складала в свою чергу 72 та 71 % для останнього циклу.

Зразки, що випробовувались у розчинах з вольфраматом, мали значно менший час освітлення – 40–50 с, у порівнянні з 360 с у зразка, який випробували у чистому розчині 0,1 М КОН.

Також був запропонований можливий механізм, що пояснює відмінності у поведінці різних зразків.

Ключові слова: електрохромізм, електроосадження, інтеркаляція, $Ni(OH)_2$, гідроксид нікелю, вольфрамат, WO_4^{2-}, полівініловий спирт

UDC 544.653.1
DOI: 10.15587/1729-4061.2018.145223

A STUDY OF THE EFFECT OF TUNGSTATE IONS ON THE ELECTROCHROMIC PROPERTIES OF $Ni(OH)_2$ FILMS

V. Kotok
PhD, Associate Professor
Department of Processes, Apparatus and General Chemical Technology*
E-mail: valeriykotok@gmail.com
PhD, Associate Professor
Department of Technologies of Inorganic Substances and Electrochemical Manufacturing**
V. Kovalenko
PhD, Associate Professor
Department of Analytical Chemistry and Chemical Technologies of Food Additives and Cosmetics*
E-mail: vadimchem@gmail.com
PhD, Associate Professor
Department of Technologies of Inorganic Substances and Electrochemical Manufacturing**
*Ukrainian State University of Chemical Technology
Gagarina ave, 8, Dnipro, Ukraine, 49005
** Vyatka State University
Moskovskaya str., 36, Kirov, Russian Federation, 610000

1. Introduction

Smart devices are a new class of devices that tend to be a combination of standard device and computer. Such combination allows for expansion of device's functionality. Use of these devices opens a wide range of possibilities for rational use of time and energy resources [1, 2]. This becomes possible due to flexible operation schedule, including switching based sensor readouts or other information passed to the computer [3].

Smart windows are a type of smart devices that can alter their optical characteristics: color, glossiness, reflection coefficient, transparency. The application range of such windows is wide. Patient examination rooms, business meeting rooms, glassing of cars, planes, modern buildings, displays for currency, prices, temperature – is a far from complete list of applications for such devices [4, 5].

The core component of a smart window is an electrochromic element. Such elements employ different systems, including systems based on liquid crystals (LC) [6, 7], suspended particles (SP) [8, 9], and electrochemical electrochromic systems [10, 11].

Electrochemical electrochromic systems change their optical properties as a result of reversible electrochemical reaction, with at least one compound having intense coloration. These systems are significantly cheaper than LC or SP systems, but also have a set of drawbacks. Relatively slow color switching and insufficient durability limit the application of electrochemical electrochromic systems.

One of the materials for electrochemical electrochromic films is nickel (II) hydroxide. Its thin films are transparent and can undergo electrochemical coloration to dark-brown, according to the reaction (1):

$$Ni(OH)_2 \leftrightarrow NiOOH+H^++\bar{e}, \quad (1)$$

where $Ni(OH)_2$ – transparent, NiOOH – dark-brown.

The prospect of mass production of smart windows with this material is rather high, owing to its good specific characteristics. However, instability of operation parameters of this material [12, 13] and slow color switching limits its application.

Thus, successful application of this material calls for scientific groups to work on a solution for these problems.

2. Literature review and problem statement

$Ni(OH)_2$ is a compound that found application in various devices. It is used as active material in alkaline accumulators [14, 15] and hybrid supercapacitors [16, 17]. Nickel hydroxide co-precipitated with some metals can be used for various purposes. Electrodes with such compounds can be used to create effective water decomposition electrolyzers [18] and for oxidation of some organic compounds, including methanol in fuel cells [19]. $Ni(OH)_2$, deposited as a thin film [20, 21] onto a conductive transparent substrate can be used in electrochromic elements of smart windows as an anodic electrochrome.

Various approaches to improve the characteristics of this material have been proposed by researchers. One approach is the creation of effective composite materials. For instance, the paper [22] proposes a composite of nickel hydroxide with reduced graphene oxide, which showed excellent electrochromic properties and can be used in accumulators and sensors. Other authors [23] propose a nanocomposite containing nickel oxide with lithium and zirconium, which posses optimal electrochromic characteristics: 30 cm^2/C (λ=670 nm).

Another approach is the formation of nanostructured (0D, 1D, 2D, 3D) films [24], inducing nickel-based ones. Such films posses better permeability, resulting in better performance.

One way to improve the characteristics of nickel hydroxide, as an anodic electrochrome, is doping with different metals and formation of nickel-based layered double hydroxides (LDH). For instance, the papers [26, 27] describe deposition of Ni-Al with rather high characteristics: high switching speed (2–4 s), 96 % transparency and low degradation rate.

A fundamentally different approach is a synthesis of nickel hydroxide compounds intercalated with large ions. Thus, researchers [28] describe intercalation of $Fe(CN)_6]^{4-}$, $[Ru(CN)_6]^{4-}$, $[Mo(CN)_8]^{4-}$ and $[IrCl_6]^{2-}$ into the lattice of Ni-Al LDH, which resulted in higher characteristics. The same team [29] also describes the improved performance of Ni-Al LDH in the presence of $[Co(bpy)_3]^{2+}$ cation, and in the other paper [30] – in the presence of ion mixtures: $[Ru(bpy)_3]^{2+}$ and $[Co(bpy)_3]^{2+}$, $[Ru(bpy)_3]^{2+}$ and $[Fe(CN)_6]^{4-}$.

Additionally, even earlier researches revealed improved electrochromic performance of $Ni(OH)_2$ when $[Fe(CN)_6]^{4-}$ was introduced to cycling electrolyte [31].

It can be summarized that some large, multivalent cations and anions, intercalated into the nickel hydroxide lattice, can improve electrochromic performance of nickel hydroxide. Considering these facts, it was decided to study the influence of WO_4^{2-} anion on electrochromic properties of nickel hydroxide. While the idea itself seemed interesting, no such data had been found in the reviewed literature [28–31].

3. The aim and objectives of the study

The aim of the work was to study the influence of WO_4^{2-} ions on electrochemical and electrochromic properties of $Ni(OH)_2$ film.

In the scope of the set aim, the following objectives were set:

– to prepare electrochromic $Ni(OH)_2$ films, using the cathodic template deposition method;

– to conduct a comparative analysis of electrochemical and electrochromic characteristics of films cycled in the electrolyte with and without WO_4^{2-}.

4. Materials and methods used in the study

Materials and reagents used in experiments

Analytical grade reagents were used in all experiments. K_2WO_4 was chosen as a source of tungstate ions so as not to introduce any other ions to the KOH cyclic electrolyte.

Glass slides coated with fluorine-doped tin oxide (FTO) (10 Ω/□), with the working area of 20×20 mm were used as a substrate for deposition of nickel hydroxide films.

Electrolyte composition used for film deposition and deposition conditions are listed in Table 1. Deposition was carried out with nickel anode [13, 32]. The thickness of the films deposited under such conditions was about 140 nm [13].

Table 1

Deposition conditions for preparation of electrochromic films using the cathodic template method

Electrolyte composition	Electrolyte temperature, °C	Cathodic current density, mA/cm^2	Deposition time, min
1. $Ni(NO_3)_2$ – 0.1 mole/L 2. Polyvinyl alcohol (PVA) – 50 g/l	30	0.1	10

The initial cycling solution was 0.1 KOH. For experiments with tungstate-containing electrolyte, three solutions with different concentrations were tested. The compositions of tested electrolytes and sample labels are listed in Table 2. Prior to cycling, each film was equilibrated with the electrolyte for 15 minutes.

Table 2

Cycling electrolyte and film labels

No.	1	2	3	4
Electrolyte	0.1 M KOH	0.1 M KOH+ +0.1 mM K_2WO_4	0.1 M KOH+ +0.3 mM K_2WO_4	0.1 M KOH+ +1 mM K_2WO_4
Label of the film cycled in this electrolyte	S	1W	3W	10W

Evaluation of electrochemical and electrochromic characteristics of deposited films. Optical and electrochemical characteristics were studied by means of cyclic voltamperometry (CVA) with simultaneous recording of the coloration-bleaching process, using a cell depicted in Fig. 1.

Ag/AgCl (KCl sat.) was used as a reference electrode and nickel foil was used as a counter-electrode. Optical characteristics were recorded at a rate of 3 Hz using the analog-to-digital converter E-154 (Russia), and electrochemical measurements were conducted using the digital potentiostat-galvanostat Ellins P-8 (Russia).

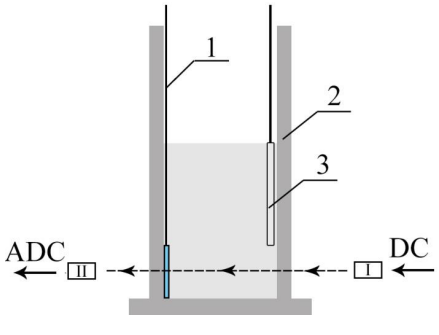

Fig. 1. Cell of optical and electrochemical tests with the electrode: 1 – working electrode with film deposition onto FTO glass; 2 – cell frame made from transparent plastic; 3 – counter-electrode; I – source of white light (5500 K); II – photoresistor. DC – source of stabilized DC voltage; ADC – analog-to-digital converter

Testing regime: potential window +200 to +725 (+900) mV, scan rate 1 mV/s, number of cycles – 5. Such number of cycles was chosen based on the literature [11–13, 20, 31, 32], and also because such number of cycles was sufficient to evaluate the influence of electrolyte additive. Positions of the peaks and their values on CVA curves were analyzed, along with any differences between cycles.

Based on the analysis of coloration-bleaching curves, the absolute coloration depth was derived, as a difference of transparency in the bleached and colored state. The shape of the curve and coloration time were also analyzed.

5. Analysis and comparison of electrochemical and optical properties of samples cycled in solutions of KOH and KOH with K_2WO_4

Fig. 2–5 show cyclic voltamperometry curves for all samples. Analysis of these curves allows to conclude that electrochemical characteristics of all samples differ significantly.

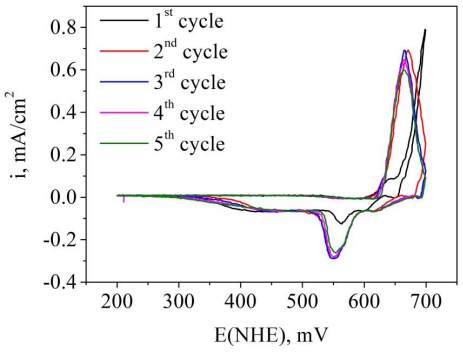

Fig. 2. Cyclic voltamperometry curve of sample S (5 cycles)

Sample S, which was cycled in pure KOH, showed a relatively low cathodic peak value (≈0.3 mA/cm^2, 3–5 cycle), and a plateau from 350 to 625 mV. While the anodic peak value is significantly higher (≈0.7 mA/cm^2, 3–5 cycle) at a potential of 665 mV.

At the same time, the cyclic voltamperometry curve of sample 1W, which was cycled in the electrolyte with minimum studied concentration of tungstate showed a significantly different behavior. The cathodic peak is sharp, without any plateaus, with a peak value of ≈0.5 mAcm^2. The anodic peak is higher and situated at more positive values: ≈0.8 mAcm^2, 675 mV.

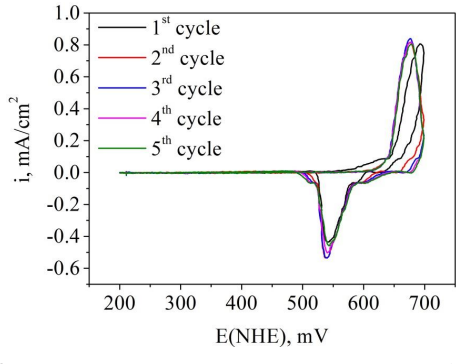

Fig. 3. Cyclic voltamperometry curve of sample 1W (5 cycles)

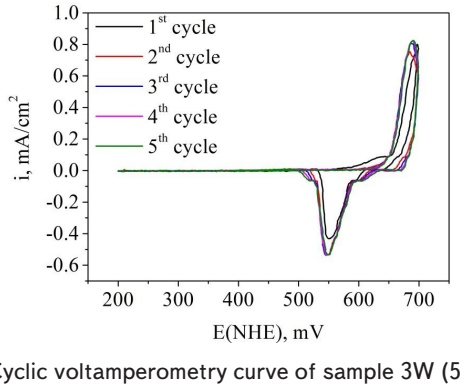

Fig. 4. Cyclic voltamperometry curve of sample 3W (5 cycles)

CVA of samples 3W and 10W (Fig. 4, 5) also significantly differ from the initial sample S. Cathodic peak current densities are about 0.5 mA/cm^2, which is significantly higher than that of the initial sample. Anodic peak current densities are about equal and are ≈0.8 mA/cm^2.

Additionally, higher tungstate concentrations in the cycling electrolyte also affected the position of the oxidation peak, shifting it toward more positing potentials. Thus, with increasing tungstate concentration for samples 1W, 3W and 10W, the anodic peak shifted from 675 mV to 683 mV, and further to 691 mV. With the anodic peak potential for sample S being 665 mV.

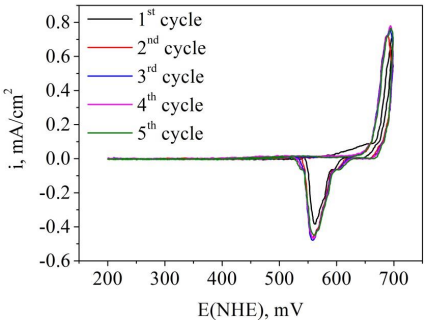

Fig. 5. Cyclic voltamperometry curve of sample 10W (5 cycles)

A similar potential shift with increasing WO_4^{2-} concentration was also observed for the cathodic peak: 535 mV, 550 mV and 560 mV. Thus, it can be seen that even small concentrations of tungstate have a significant influence on electrochemical processes within the $Ni(OH)_2$ film, which is also reflected in the optical behavior.

Optical characteristics obtained for all samples are shown in Fig. 6–10.

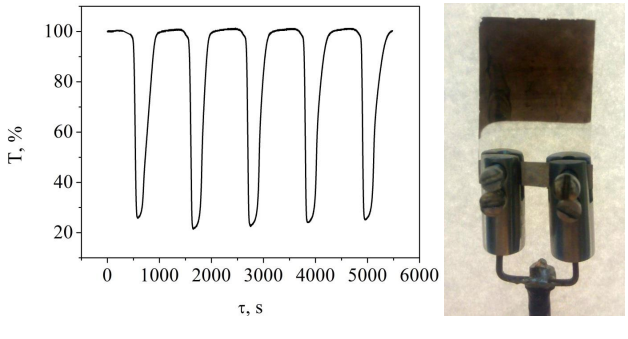

a *b*

Fig. 6. Results for sample S: *a* — coloration-bleaching curve; *b* — photograph of the film in the colored state after cycling

Value "T" (Fig. 6, *a*) is transparency, relative to the non-transparent electrode, expressed as a percentage, τ is time. For illustration, there is also a photograph of the colored electrode after cycling, with uniform backlighting. Because the overall shape of coloration-bleaching curves for all samples was the same, with notable differences observable under magnification, the curves of other samples have been omitted.

In order to analyze changes in the absolute coloration degree during cycling, the values (*D*, %) were plotted against the cycle number for each sample – Fig. 7. For a more detailed analysis of coloration-bleaching curves, a zoomed combined graph, showing the last cycle for all samples, was plotted – Fig. 8.

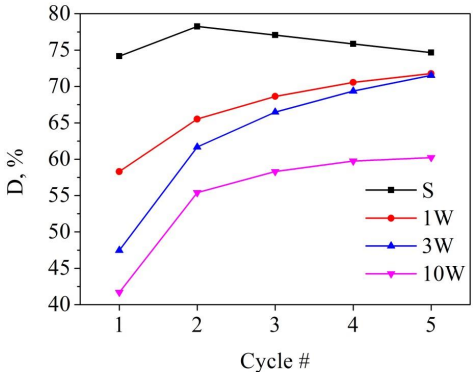

Fig. 7. Coloration degree values plotted against the cycle number for all samples

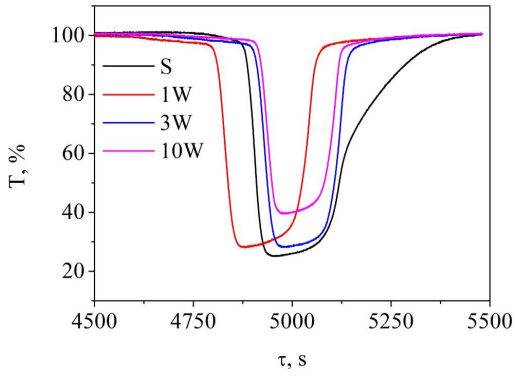

Fig. 8. Last coloration-bleaching cycle for all samples

Analysis of these dependencies revealed that the initial sample S has the highest absolute coloration degree of 74 % for all cycles. Nevertheless, sample 1W and 3W are almost equal with sample S, in terms of absolute coloration degree at later cycles – 72 and 71 % respectively. Only sample 10W showed a significant decrease of this characteristic – 60 %. An interesting occurrence is that curves of all samples cycled in the tungstate-containing electrolyte (samples 1W, 3W, 10W) had similar behavior. At first, there was a significant increase in the absolute coloration degree (cycles 1–2), with a lower increase for subsequent cycles. Sample S, cycled without tungstate, shows a different behavior – some initial increase, with gradual degradation of the absolute coloration value afterwards.

Analysis of bleaching-coloration curves revealed that all curves have a similar shape, with the exception of sample S, which bleaches notably slower (curve region from 5110 to 5450 s). This means that bleaching time is longer, in comparison to samples cycled in tungstate-containing electrolytes. The time for complete bleaching in the pure electrolyte is estimated to be about 360 s, while for tungstate-containing electrolytes it is about 40–50 seconds.

6. Discussion of experimental data for electrochromic films cycled in electrolytes with and without tungstate ions

As a result of conducted experiments, it was discovered that small concentrations of tungstate ions have an effect on

electrochemical and electrochromic characteristics of films. This results in better reversibility of electrodes – specific peak currents of oxidation and reduction become closer in their values. Presence of WO_4^{2-} results in a sharper cathodic peak and disappearance of the current plateau. Nevertheless, increase of tungstate concentration in cycling electrolyte results in a shift of cathodic and anodic peak potentials to more positive values. This is related to changes in the equilibrium potential, which in turn, supposedly, changed because of structural changes of electrochromic material. Our assumption is that the exchange of ions that reside between the layers of the (001) plane occurs, similar to what's been described in the literature [28–31, 33]. It should be noted that for $Ni(OH)_2$ [34] and nickel-based LDH [26,27, 35–38], the ions of source salts can reside between the layers in the direction of the (001) plane. It is known that for nickel hydroxide, electrochemically prepared from nickel nitrate, these are nitrate ions [34]. NO_3^- can be exchanged for other ions. We assume that exchange of nitrate for tungstate occurs, similar to intercalation that occurs with the cathode in lithium batteries [39, 40]. Due to the larger size of WO_4^{2-}, a greater deformation occurs in the crystal lattice, resulting in the potential shift. The proposed mechanism is illustrated in Fig. 9. The structural changes also result affect the properties of the electrochromic film.

It is also assumed that intercalation occurs during contact with the electrolyte and as a part of the cycling process. This is implied by two facts. Firstly, the bleaching rate of samples 1W, 3W and 10W exceed that of sample S by the second cycle. This indicates partial intercalation and activation of electrochromic films during contact with the tungstate-containing electrolyte. Secondly, different behavior of optical curves for the samples cycled in electrolytes with and without electrolytes, which was discussed in paragraph 5. The later indicates further intercalation of tungstate ions during film cycling. It is worth to note that the intercalation process can occur rather quickly, which was described in the literature [41, 42]. It is described that the intercalation process into the crystal lattice of nickel hydroxide can occur for 60 and 30 min respectively. This supports the possibility of partial intercalation of WO_4^{2-} into films during its equilibration with electrolyte, which was 15 min. It should also be noted that introduction of anions can improve specific characteristics of nickel hydroxide. For instance, it is shown [43, 44] that intercalation of polyoxyvanadate and carbonate ions can significantly improve the characteristics of nickel hydroxide.

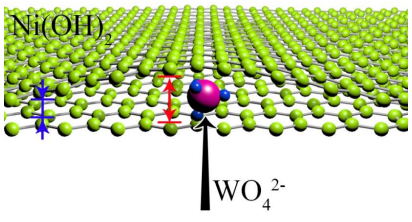

Fig. 9. Schematic illustration of WO_4^{2-} intercalation and of the crystal lattice of $Ni(OH)_2$. Oxygen and hydrogen atoms are omitted for simplification

The most pronounced effect from tungstate ion was a decrease of bleaching time, which resulted in lower bleaching time from 360 to 40–50 s.

Thus, introduction of small amounts of WO_4^{2-} can improve bleaching rate and can possibly improve electrochromic characteristics. The latter assumption, along with the assumed mechanism, requires additional studies, which will be conducted in future works.

7. Conclusions

1. As a result of the work, it was discovered that the introduction of small concentrations (0.1–1 mM) of WO_4^{2-} ions into cycling electrolyte can lead to significant changes in electrochemical and electrochromic characteristics of nickel hydroxide films. This also resulted in a higher bleaching rate.

2. The optimal concentration of WO_4^{2-} was found to be 0.1 mM, which resulted in a decrease of bleaching time to 50 s, with the absolute coloration degree of 72 %. At the same time, the film cycled in pure alkaline electrolyte showed bleaching time of 360 s with the absolute coloration degree of 74 %.

References

1. Smart Windows: Energy Efficiency with a View. URL: https://www.nrel.gov/news/features/2010/1555.html
2. Risteska Stojkoska B. L., Trivodaliev K. V. A review of Internet of Things for smart home: Challenges and solutions // Journal of Cleaner Production. 2017. Vol. 140. P. 1454–1464. doi: https://doi.org/10.1016/j.jclepro.2016.10.006
3. Silverio-Fernández M., Renukappa S., Suresh S. What is a smart device? – a conceptualisation within the paradigm of the internet of things // Visualization in Engineering. 2018. Vol. 6, Issue 1. doi: https://doi.org/10.1186/s40327-018-0063-8
4. A Review of Electrochromic Windows for Residential Applications / Sibilio S., Rosato A., Scorpio M., Iuliano G., Ciampi G., Vanoli G., de Rossi F. // International Journal of Heat and Technology. 2016. Vol. 34. P. S481–S488. doi: https://doi.org/10.18280/ijht.34s241
5. All-in-One Gel-Based Electrochromic Devices: Strengths and Recent Developments / Alesanco Y., Viñuales A., Rodriguez J., Tena-Zaera R. // Materials. 2018. Vol. 11, Issue 3. P. 414. doi: https://doi.org/10.3390/ma11030414
6. A greener electrochromic liquid crystal based on ionic liquid electrolytes / He Z., Yuan X., Zhao Y., Zou C., Guo S., He B. et. al. // Liquid Crystals. 2016. Vol. 43, Issue 8. P. 1110–1119. doi: https://doi.org/10.1080/02678292.2016.1160296
7. The electro-optical and electrochromic properties of electrolyte-liquid crystal dispersions / Cupelli D., De Filpo G., Chidichimo G., Nicoletta F. P. // Journal of Applied Physics. 2006. Vol. 100, Issue 2. P. 024515. doi: https://doi.org/10.1063/1.2219696
8. Electrooptical behaviour and control of a suspended particle device / Vergaz R., Pena J., Barrios D., Pérez I., Torres J. // Opto-Electronics Review. 2007. Vol. 15, Issue 3. P. 154–158. doi: https://doi.org/10.2478/s11772-007-0013-9

9. Ghosh A., Norton B., Duffy A. First outdoor characterisation of a PV powered suspended particle device switchable glazing // Solar Energy Materials and Solar Cells. 2016. Vol. 157. P. 1–9. doi: https://doi.org/10.1016/j.solmat.2016.05.013
10. Browne M. P. Electrochromic Nickel Oxide Films for Smart Window Applications // International Journal of Electrochemical Science. 2016. P. 6636–6647. doi: https://doi.org/10.20964/2016.08.38
11. Effect of deposition time on properties of electrochromic nickel hydroxide films prepared by cathodic template synthesis / Kotok V. A., Kovalenko V. L., Solovov V. A., Kovalenko P. V., Ananchenko B. A. // ARPN Journal of Engineering and Applied Sciences. 2018. Vol. 13, Issue 9. P. 3076–3086.
12. Advanced electrochromic Ni(OH)2/PVA films formed by electrochemical template synthesis / Kotok V. A., Kovalenko V. L., Kovalenko P. V., Solovov V. A., Deabate S., Mehdi A. et. al. // ARPN Journal of Engineering and Applied Sciences. 2017. Vol. 12, Issue 13. P. 3962–3977.
13. Soft Electrochemical Etching of FTO-Coated Glass for Use in Ni(OH)2-Based Electrochromic Devices / Kotok V. A., Malyshev V. V., Solovov V. A., Kovalenko V. L. // ECS Journal of Solid State Science and Technology. 2017. Vol. 6, Issue 12. P. P772–P777. doi: https://doi.org/10.1149/2.0071712jss
14. Fabrications of High-Capacity Alpha-Ni(OH)2 / Young K.-H., Wang L., Yan S., Liao X., Meng T., Shen H., Mays W. // Batteries. 2017. Vol. 3, Issue 4. P. 6. doi: https://doi.org/10.3390/batteries3010006
15. Kovalenko V., Kotok V. Definition of effectiveness of β-$Ni(OH)_2$ application in the alkaline secondary cells and hybrid supercapacitors // Eastern-European Journal of Enterprise Technologies. 2017. Vol. 5, Issue 6 (89). P. 17–22. doi: https://doi.org/10.15587/1729-4061.2017.110390
16. Assembly of $Ni(OH)_2$-graphene hybrids with a high electrochemical performance by a one-pot hydrothermal method / Yuan B., Zheng X., Zhang C., Lu W., Li B., Yang Q.-H. // New Carbon Materials. 2014. Vol. 29, Issue 6. P. 426–431. doi: https://doi.org/10.1016/s1872-5805(14)60147-5
17. Kotok V., Kovalenko V. The properties investigation of the faradaic supercapacitor electrode formed on foamed nickel substrate with polyvinyl alcohol using // Eastern-European Journal of Enterprise Technologies. 2017. Vol. 4, Issue 12 (88). P. 31–37. doi: https://doi.org/10.15587/1729-4061.2017.108839
18. Superaerophobic P-doped Ni(OH)2/NiMoO4 hierarchical nanosheet arrays grown on Ni foam for electrocatalytic overall water splitting / Xi W., Yan G., Tan H., Xiao L., Cheng S., Khan S. U. et. al. // Dalton Transactions. 2018. Vol. 47, Issue 26. P. 8787–8793. doi: https://doi.org/10.1039/c8dt00765a
19. Highly active and durable methanol oxidation electrocatalyst based on the synergy of platinum–nickel hydroxide–grapheme / Huang W., Wang H., Zhou J., Wang J., Duchesne P. N., Muir D. et. al. // Nature Communications. 2015. Vol. 6, Issue 1. doi: https://doi.org/10.1038/ncomms10035
20. Kotok V., Kovalenko V. The electrochemical cathodic template synthesis of nickel hydroxide thin films for electrochromic devices: role of temperature // Eastern-European Journal of Enterprise Technologies. 2017. Vol. 2, Issue 11 (86). P. 28–34. doi: https://doi.org/10.15587/1729-4061.2017.97371
21. Electrochromic properties of sol–gel prepared hybrid transition metal oxides – A short review / Jittiarporn P., Badilescu S., Al Sawafta M. N., Sikong L., Truong V.-V. // Journal of Science: Advanced Materials and Devices. 2017. Vol. 2, Issue 3. P. 286–300. doi: https://doi.org/10.1016/j.jsamd.2017.08.005
22. One material, multiple functions: graphene/$Ni(OH)_2$ thin films applied in batteries, electrochromism and sensors / Neiva E. G. C., Oliveira M. M., Bergamini M. F., Marcolino L. H., Zarbin A. J. G. // Scientific Reports. 2016. Vol. 6, Issue 1. doi: https://doi.org/10.1038/srep33806
23. Electrochromic performance of nanocomposite nickel oxide counter electrodes containing lithium and zirconium / Lin F., Montano M., Tian C., Ji Y., Nordlund D., Weng T.-C. et. al. // Solar Energy Materials and Solar Cells. 2014. Vol. 126. P. 206–212. doi: https://doi.org/10.1016/j.solmat.2013.11.023
24. Recent Advances in Electrochromic Smart Fenestration / Cai G., Eh A. L.-S., Ji L., Lee P. S. // Advanced Sustainable Systems. 2017. Vol. 1, Issue 12. P. 1700074. doi: https://doi.org/10.1002/adsu.201700074
25. Ma D., Wang J. Inorganic electrochromic materials based on tungsten oxide and nickel oxide nanostructures // Science China Chemistry. 2016. Vol. 60, Issue 1. P. 54–62. doi: https://doi.org/10.1007/s11426-016-0307-x
26. Electrodeposition of Ni-Al layered double hydroxide thin films having an inversed opal structure: Application as electrochromic coatings / Martin J., Jack M., Hakimian A., Vaillancourt N., Villemure G. // Journal of Electroanalytical Chemistry. 2016. Vol. 780. P. 217–224. doi: https://doi.org/10.1016/j.jelechem.2016.09.022
27. Aluminum doped nickel oxide thin film with improved electrochromic performance from layered double hydroxides precursor in situ pyrolytic route / Shi J., Lai L., Zhang P., Li H., Qin Y., Gao Y. et. al. // Journal of Solid State Chemistry. 2016. Vol. 214. P. 1–8. doi: https://doi.org/10.1016/j.jssc.2016.05.032
28. Mondal D., Villemure G. Improved reversibility of color changes in electrochromic Ni–Al layered double hydroxide films in presence of electroactive anions // Journal of Electroanalytical Chemistry. 2012. Vol. 687. P. 58–63. doi: https://doi.org/10.1016/j.jelechem.2012.09.046
29. Mondal D., Villemure G. Effect of the presence of on the electrochromic responses of films of a redox active Ni–Al-layered double hydroxide // Journal of Electroanalytical Chemistry. 2009. Vol. 628, Issue 1-2. P. 67–72. doi: https://doi.org/10.1016/j.jelechem.2009.01.007

30. Mondal D., Jack M., Villemure G. Improved contrast between the coloured and transparent states in electrochromic Ni–Al layered double hydroxide films in mixtures of electroactive ions // Journal of Electroanalytical Chemistry. 2014. Vol. 722-723. P. 7–14. doi: https://doi.org/10.1016/j.jelechem.2014.02.025
31. Smart windows: cation internal and anion external activation for electrochromic films of nickel hydroxide / Kotok V. A., Malahova E. V., Kovalenko V. L., Baramzin M. N., Kovalenko P. V.; V. Z. Barsukov, Yu. V. Borysenko, O. I. Buket, V. G. Khomenko (Eds.) // Promising materials and processes in technical electrochemistry. Kyiv: KNUTD, 2016. P. 224–228.
32. Kotok V., Kovalenko V. Investigation of the electrochromic properties of $Ni(OH)_2$ films on glass with ITONi bilayer coating // Eastern-European Journal of Enterprise Technologies. 2018. Vol. 3, Issue 5 (93). P. 55–61. doi: https://doi.org/10.15587/1729-4061.2018.133387
33. Carpani I. Study on the intercalation of hexacyanoferrate(II) in a Ni, Al based hydrotalcite // Solid State Ionics. 2004. Vol. 168, Issue 1-2. P. 167–175. doi: https://doi.org/10.1016/j.ssi.2004.01.032
34. Jayashree R. S., Vishnu Kamath P. Factors governing the electrochemical synthesis of α-nickel (II) hydroxide // Journal of Applied Electrochemistry. 1999. Vol. 29, Issue 4. P. 449–454. doi: https://doi.org/10.1023/a:1003493711239
35. Kovalenko V., Kotok V. Obtaining of Ni–Al layered double hydroxide by slit diaphragm electrolyzer // Eastern-European Journal of Enterprise Technologies. 2017. Vol. 2, Issue 6 (86). P. 11–17. doi: https://doi.org/10.15587/1729-4061.2017.95699
36. Kovalenko V., Kotok V. Study of the influence of the template concentration under homogeneous precepitation on the properties of Ni(OH)2 for supercapacitors // Eastern-European Journal of Enterprise Technologies. 2017. Vol. 4, Issue 6 (88). P. 17–22. doi: https://doi.org/10.15587/1729-4061.2017.106813
37. Synthesis and characterisation of dyeintercalated nickelaluminium layereddouble hydroxide as a cosmetic pigment / Kovalenko V., Kotok V., Yeroshkina A., Zaychuk A. // Eastern-European Journal of Enterprise Technologies. 2017. Vol. 5, Issue 12 (89). P. 27–33. doi: https://doi.org/10.15587/1729-4061.2017.109814
38. Kotok V., Kovalenko V., Vlasov S. Investigation of NiAl hydroxide with silver addition as an active substance of alkaline batteries // Eastern-European Journal of Enterprise Technologies. 2018. Vol. 3, Issue 6 (93). P. 6–11. doi: https://doi.org/10.15587/1729-4061.2018.133465
39. Porous LiMn2O4 Microspheres With Different Pore Size: Preparation and Application as Cathode Materials for Lithium Ion Batteries / Li S., Zhu K., Liu J., Zhao D., Cui X. // Journal of Electrochemical Energy Conversion and Storage. 2018. Vol. 16, Issue 1. P. 011006. doi: https://doi.org/10.1115/1.4040567
40. Enhanced Electrochemical Properties of Zr4+-doped Li1.20[Mn0.52Ni0.20Co0.08]O2 Cathode Material for Lithium-ion Battery at Elevated Temperature / Lu Y., Pang M., Shi S., Ye Q., Tian Z., Wang T. // Scientific Reports. 2018. Vol. 8, Issue 1. doi: https://doi.org/10.1038/s41598-018-21345-6
41. Lee J. W., Ko J. M., Kim J.-D. Hierarchical Microspheres Based on α-$Ni(OH)_2$ Nanosheets Intercalated with Different Anions: Synthesis, Anion Exchange, and Effect of Intercalated Anions on Electrochemical Capacitance // The Journal of Physical Chemistry C. 2011. Vol. 115, Issue 39. P. 19445–19454. doi: https://doi.org/10.1021/jp206379h
42. Crepaldi E. L., Pavan P. C., Valim J. B. A new method of intercalation by anion exchange in layered double hydroxides // Chemical Communications. 1999. Issue 2. P. 155–156. doi: https://doi.org/10.1039/a808567f
43. Kovalenko V., Kotok V., Bolotin O. Definition of factors influencing on Ni(OH)2 electrochemical characteristics for supercapacitors // Eastern-European Journal of Enterprise Technologies. 2016. Vol. 5, Issue 6 (83). P. 17–22. doi: https://doi.org/10.15587/1729-4061.2016.79406
44. Direct growth of 2D nickel hydroxide nanosheets intercalated with polyoxovanadate anions as a binder-free supercapacitor electrode / Gunjakar J. L., Inamdar A. I., Hou B., Cha S., Pawar S. M., Abu Talha A. A. et. al. // Nanoscale. 2018. Vol. 10, Issue 19. P. 8953–8961. doi: https://doi.org/10.1039/c7nr09626g